


# All-fiber erbium-doped dissipative soliton laser with multimode interference based on saturable-reserve saturable hybrid optical switch

Xin Zhao(赵鑫), Renyan Wan(王仁严), Weiyan Li(李卫岩), Liang Jin(金亮), He Zhang(张贺), Yan Li(李岩), Yingtian Xu(徐英添), Linlin Shi(石琳琳), and Xiaohui Ma(马晓辉)

**Citation:**Chin. Phys. B, 2022, 31 (**6**): 064215. DOI: 10.1088/1674-1056/ac5611
Journal homepage: http://cpb.iphy.ac.cn; http://iopscience.iop.org/cpb

**What follows is a list of articles you may be interested in**

---

## Independently tunable dual resonant dip refractive index sensor based on metal—insulator—metal waveguide with Q-shaped resonant cavity

Haowen Chen(陈颢文), Yunping Qi(祁云平), Jinghui Ding(丁京徽), Yujiao Yuan(苑玉娇), Zhenting Tian(田振廷), and Xiangxian Wang(王向贤)
Chin. Phys. B, 2022, 31 (**3**): 034211. DOI: 10.1088/1674-1056/ac48fe

## Tunable characteristic of phase-locked quantum cascade laser arrays

Zeng-Hui Gu(顾增辉), Jin-Chuan Zhang(张锦川), Huan Wang(王欢), Peng-Chang Yang(杨鹏昌), Ning Zhuo(卓宁), Shen-Qiang Zhai(翟慎强), Jun-Qi Liu(刘俊岐), Li-Jun Wang(王利军), Shu-Man Liu(刘舒曼), Feng-Qi Liu(刘峰奇), and Zhan-Guo Wang(王占国)
Chin. Phys. B, 2021, 30 (**10**): 104201. DOI: 10.1088/1674-1056/abec30

## Unitary transformation of general nonoverlapping-image multimode interference couplers with any input and output ports

Ze-Zheng Li(李泽正), Wei-Hua Han(韩伟华), Zhi-Yong Li(李智勇)
Chin. Phys. B, 2020, 29 (**1**): 014206. DOI: 10.1088/1674-1056/ab5783

## High-performance waveguide-integrated Ge/Si avalanche photodetector with small contact angle between selectively epitaxial growth Ge and Si layers

Xiao-Qian Du(杜小倩), Chong Li(李冲), Ben Li(黎奔), Nan Wang(王楠), Yue Zhao(赵越), Fan Yang(杨帆), Kai Yu(余凯), Lin Zhou(周琳), Xiu-Li Li(李秀丽), Bu-Wen Cheng(成步文), Chun-Lai Xue(薛春来)
Chin. Phys. B, 2019, 28 (**6**): 064208. DOI: 10.1088/1674-1056/28/6/064208

## Compact 2×2 parabolic multimode interference thermo-optic switches based on fluorinated photopolymer

Ji-Hou Wang(王继厚), Chang-Ming Chen(陈长鸣), Ke-Wei Hu(胡珂玮), Ru Cheng(程儒), Chun-Xue Wang(王春雪), Yun-Ji Yi(衣云骥), Xiao-Qiang Sun(孙小强), Fei Wang(王菲), Zhi-Yong Li(李智勇), Da-Ming Zhang(张大明)
Chin. Phys. B, 2019, 28 (**4**): 044207. DOI: 10.1088/1674-1056/28/4/044207

---

# All-fiber erbium-doped dissipative soliton laser with multimode interference based on saturable-reserve saturable hybrid optical switch

Xin Zhao(赵鑫)†, Renyan Wan(王仁严), Weiyan Li(李卫岩), Liang Jin(金亮), He Zhang(张贺), Yan Li(李岩), Yingtian Xu(徐英添), Linlin Shi(石琳琳), and Xiaohui Ma(马晓辉)

*National Key Laboratory on High-Power Semiconductor Lasers, Changchun University of Science and Technology, Changchun 130022, China*

(Received 19 October 2021; revised manuscript received 5 February 2022; accepted manuscript online 17 February 2022)

Reverse saturable absorption is essential for the realization of dissipative solitons. In this paper, we introduce reverse saturable absorption by using nonlinear multimode interference (NL-MMI), for the first time, to the best of our knowledge, and obtain a stable dissipative soliton operation. By adjusting the coupling efficiency from multimode fiber to single mode fiber, the absorption properties of NL-MMI can be switched between saturation and reverse saturation. The dissipative soliton can be obtained with pulse width of 975 fs in the experiment, the 3-dB bandwidth at 1555 nm is 16 nm, and the maximum output power is 11.48 mW. The nonlinear absorption optical modulation and high damage threshold characteristics of the NL-MMI based ultrafast optical switch provide a new idea for realizing dissipative solitons.

**Keywords:** multimode interference, laser mode-locking, abnormal saturable absorption

**PACS:** 42.55.Wd **DOI:** 10.1088/1674-1056/ac5611

## 1. Introduction

Dissipative solitons (DSs) have attracted much attention due to the balance between the ultrashort pulse and large energy.[1,2] The excellent output performance is suitable for applications ranging from optical communication to ultra-precision machining.[3,4] To design a DSs fiber laser, there are several critical factors that require careful consideration. The balance among nonlinearity, dispersion, gain, and loss determines the mode-locking mechanism. Compared with the traditional soliton, the dissipative soliton is not a closed-loop system, but a dynamic balance system that continuously exchanges energy with the outside world. The dynamical balance between loss and gain is the key to a stable dissipative system. In dissipative soliton mode locking based on the two-dimensional materials, the reserve saturable absorption is realized by triggering two-photon absorption or multi-photon absorption of two-dimensional materials, but this triggering is unfavorable for generating ultrashort pulses.[5–14] Moreover, dissipative solitons based on nonlinear polarization rotation (NPR) and nonlinear optical loop mirror (NOLM) have higher damage threshold. However, the flexibility of fiber determines that these methods are vulnerable to environmental impact and lose locking.

Recently, the mode-locking based on nonlinear multimode interference (NL-MMI) has attracted attention. The principle of mode-locking based on NL-MMI is to introduce a section of multimode fiber into the oscillator, and employ the NL-MMI in multimode fiber (MMF) to control the coupling efficiency of beam from MMF to single mode fiber (SMF) to obtain nonlinear saturable absorption, and realize the mode locking.[15–19] Compared to the two-dimensional materials, the obvious superiority of NL-MMI is high optical-power thermal damage and oxidation resistance,[20] and the realization of nonlinear saturable absorption by coupling efficiency modulation means that the polarization state of beam is not required. However, the length of MMF has precise requirements for the realization of mode locking, and the modulation depth of nonlinear saturable absorption based on stretch MMF is limited, which brings great limitations to the application of mode locking based on NL-MMI.

In this paper, we obtain the tunable modulation depth based on NL-MMI optical switch from positive (saturable) to negative (reverse saturable), and realizes a stable dissipative soliton operation. By inserting two pieces of grad-index multimode fiber into an erbium-doped fiber laser, 975 fs pulse duration with 28.15 MHz repetition rate dissipative soliton is obtained, whose central wavelength is 1555 nm, and the average power is up to 11.48 mW. Dissipative soliton by combining saturable and reverse saturable absorption provides a new method for all-fiber mode-locked lasers with high energy.

## 2. The characteristics of the GIMF-based optical switch

The GIMF-based optical switch, as shown in Fig. 1, consists of a segment of GIMF (GI 50/125, YOFC), and $L$ is the length of GIMF, which is sandwiched between two segments of single mode fiber (SMF, SM28e, YOFC). Ignoring the reflected loss, the propagating light field from the SMF ex-

†Corresponding author. E-mail: zhaoxin@cust.edu.cn

© 2022 Chinese Physical Society and IOP Publishing Ltd 

cites many guided modes at the splicing point between SMF and GIMF. The excited modes in GIMF interfere with each other in the propagating process to form multimode interference (MMI), which causes the self-imaging.

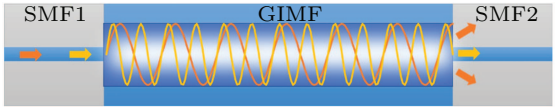



**Fig. 1.** The schematic of GIMF-based ultrafast optical switch.

The self-imaging point emerges at periodic intervals along the propagation direction of the GIMF, and $L_{\rm p}$ is the beat length, which is the distance between the two adjacent self-imaging points, $L_{\rm p} = \pi R\sqrt{2\Delta}$, while $R$ is the core radius of GIMF, and $\Delta$ is the refractive index difference between core and cladding of GIMF. By gradual increase of the injected power, the excited modes in GIMF generate phase difference due to the nonlinear birefringence, and the self-imaging point moves in the propagation direction, which causes the change in the coupling efficiency of light from GIMF to SMF. All the modes interfere with each other when they recouple back to the second section of the SMF. The SMS is coiled on PCs, and the measured relative power transmission of SMF-GIMF-SMF can be given by[21]

$$T = 1 + 2\sqrt{\kappa(1-\kappa)}\cos\left(2\pi\left(n_1 - n_2\right)L/\lambda + \varphi\right), \qquad (1)$$

where $\kappa$ is the coupling coefficient of the fundamental mode, $n_1$ and $n_2$ are refractive indexes of two modes, $L$ is the length of the multimode fiber, and $\varphi$ is the additional phase shift of the excited modes, which is caused by the nonlinear birefringence. In the experiment, the GIMF is coiled on the paddles of PC, and the $\varphi$ of GIMF can be tuned by adjusting the stress applied on the fiber by changing the orientation angle of paddles. The additional phase shift $\varphi$ can be expressed as

$$\varphi = \arctan\left(\tan\left(\delta_1 - \delta_2\right)\cos 2\Omega\right), \qquad (2)$$

where $\delta_1$ and $\delta_2$ are the stress-induced birefringence intensity of the two modes, and $\Omega$ stands for the angle of the fast axis orientation of the PC with respect to the $x$ polarization component assuming the same orientation angle for the two modes. The saturable or reverse saturable absorption of GIMF satisfies[22–24]

$$\Delta\beta_n L + \varphi = m\pi, \qquad (3)$$

where $\Delta\beta_n = \beta_i - \beta_j$, $\beta_i$ and $\beta_j$ are the propagation constants of $i$-th mode and $j$-th mode. The saturable absorption of GIMF can be excited when $m$ is odd, and reverse saturable absorption of GIMF can be excited when $m$ is even. In other word, the beat length $L_{\rm p}$ can be expressed as

$$L_{\rm p} = \frac{2\left(m\pi - \varphi\right)}{\Delta\beta_n}. \qquad (4)$$

Equation (4) indicates that the beat length $L_{\rm p}$ can be changed by adjusting the additional phase shift $\varphi$. When the length of GIMF equal to $L = mL_{\rm p}/2$ and $m$ is an odd integer, the saturable absorption can be excited. Contrarily, when $m$ is an even integer, reserve saturable absorption can be excited.[25,26] Hence, saturable or reverse saturable absorption can be achieved by adjusting the additional phase shift $\varphi$ rather than by precisely controlling the length of GIMF $L$.

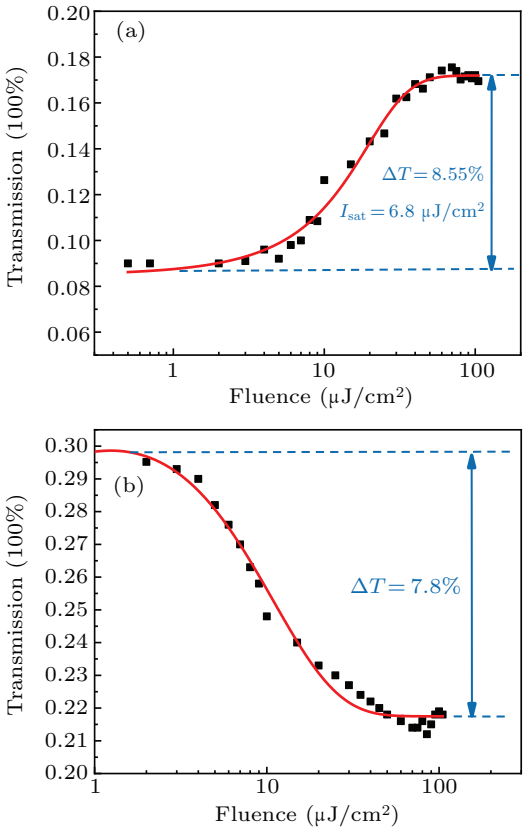



**Fig. 2.** (a) The saturable absorption curve of GIMF, (b) the reverse saturable absorption curve of GIMF.

The nonlinear transmission of GIMF is measured by I-scan experiment. A homemade mode-locked fiber laser serves as the light source, whose central wavelength is 1561.12 nm, pulse duration is $\sim$ 600 fs, and fundamental repetition rate is 25 MHz. An erbium-doped fiber amplifier (EDFA) is employed to amplify the optical pulse, by using an optical attenuator. The average power could be deliberately controlled, the output is divided into two parts by a 50:50 coupler, one part of beam are injected into GIMF, and then the powers are measured by power meters, and the pigtails of all devices are SMFs. By adjusting the paddles of PC on GIMF, two curves with saturable absorption and reverse saturable absorption can be obtained in the same GIMF, respectively, as shown in Fig. 2, which indicates the nonlinear transmittance of GIMF can be changed by adjusting the additional phase shift. In the saturable region, the transmission with the wavelength of 1561.12 nm is around 9% at the lower pulse fluence.

With the increase of pulse fluence, the maximum transmission of GIMF is around 17%, the modulation depth $\Delta T$ is about $\sim 8.55\%$, and the saturation intensity $I_{\text{sat}}$ is 6.8 μJ/cm$^2$, as shown in Fig. 2(a). In the reverse saturable region, the transmission is about 30%, by increasing the pulse fluence, the minimum transmission of GIMF can reach 22%, and the modulation depth of saturable absorber is $\Delta T_{\text{abn}} = -7.8\%$, as shown in Fig. 2(b).

## 3. Experimental setup

The experimental setup of all-fiber erbium-doped dissipative soliton laser configuration is demonstrated in Fig. 3. The laser cavity is built in a ring cavity where the mode-locking is obtained via CA-GIMFs ultrafast optical switch, a 40 cm long erbium heavily-doped fiber (Er80-8/125, Liekki) with group velocity dispersion (GVD) of $\sim$ 15 ps/nm·km as gain medium, which is simultaneously pumped by a single mode 976 nm semiconductor laser module, coupled to the ring cavity by a 980/1550 nm wavelength-division multiplexing (WDM), and the maximum output is 2 W, a section of 0.85 m length dispersion compensation fiber (DCF) with GVD of $-152.6$ ps/nm·km is added in the cavity to compensate the dispersion to the normal dispersion region. Two pieces of graded-index multimode fibers (GIMF) are introduced in the ring cavity and compose a cascaded GIMFs (CA-GIMFs) optical switch, which is used to excite the saturable absorption and reserve saturable absorption. The coupling efficiency of multimode fiber and single mode fiber is adjusted by coiling PC1 and PC2 on two GIMFs respectively. The polarization independent isolator (PI-ISO) guarantees the beam in the cavity unidirectional transmission. The generated dissipative soliton pulses are directed out by using a 90:10 coupler, and the total length of the ring cavity is 6.87 m. The pulses are simultaneously monitored by an optical spectrum analyzer (AQ6370D, Yokogawa) with the accuracy of 0.02 nm, and an autocorrelation (FR-103XL, Femtochrome) connected to an oscilloscope (DSOV084A, Keysight).

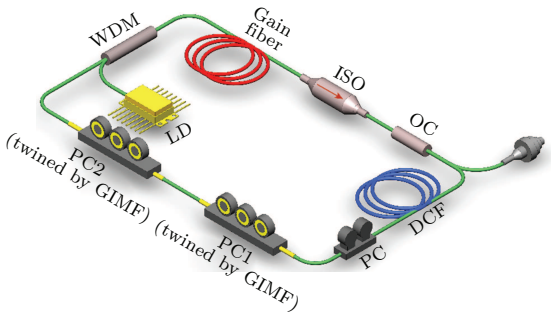



**Fig. 3.** Structure of positive dispersion mode-locked fiber laser.

## 4. Result and discussion

By fine adjustment of PC1 and PC2, the dissipative soliton can be observed at the threshold of 400 mW, in the normal dispersion regime. Figure 5(a) indicates the spectrum of DSs, the center wavelength is 1555 nm, and the edge-to-edge of the spectrum width is 15 nm. The spectrum demonstrates steep side edges, which indicates the typical characteristics of dissipative solitons. The pulse width of $\sim$ 975 fs is observed in Fig. 5(b), the pulse train are displayed in Fig. 5(c), and the corresponding repetition rate is 28.15 MHz. The evolution of DSs along the propagation direction in CA-GIMFs can be represented in Fig. 4, which can be divided into five stages. Firstly, the beam in SMF is transmitted in the form of continuous wave, and the fluctuation of light intensity is random. When the beam incident into GIMF, the high-order modes are excited and coupling between different mode forms periodic self-imaging points in GIMF, in the second stage. However, the peak power of the initial pulse is not fixed but changes periodically due to the net positive dispersion of the cavity. When the beam enters SMF from GIMF, it makes the beginning of the third stage. By adjusting the paddles of PC1, the additional phase shift $\varphi$ can be modulated to satisfy the condition of saturable absorption, and the pulse train with peak power changed periodically propagates in SMF2. When the pulse train propagates to GIMF2, the MMI also excites periodic self-imaging points, PC2 is finely adjusted to make the introduced additional phase $\varphi$ satisfy the reverse saturable absorption, the pulses with high peak power are clamped and make the pulse train have a uniform peak power. The dissipative soliton is with the maximum average power of 11.48 mW at the pump power of 800 mW, which corresponding to the pulse energy is 0.41 nJ.

In order to verify the effect of reverse saturable absorption on the establishment of dissipative solitons, we remove the GIMF2 with reverse absorption part from the cavity. By adjusting the paddles of PC and PC1, the pulse train with periodic fluctuation intensity are observed at the threshold pump power of 400 mW, which possess the characteristics of dispersion-managed soliton, and no dissipative soliton or harmonic mode-locking can be obtained by increasing the pump power up or adjusting the paddles of PCs. The spectrum and pulse train of output at pump power of 800 mW are shown in Fig. 6. The central wavelength remains unchanged at 1555 nm, but the 3-dB bandwidth of the spectrum is narrowed to 1 nm, as shown in Fig. 6(a). It should be noted that some satellite-peaks are symmetrically distributed on both sides of the main peak, which indicates the existence of periodically modulated pulses in the cavity. Figure 6(b) records the dispersion-managed soliton pulse train, and Fig. 6(c) shows

the details by zooming-in the horizontal coordinate. The pulse width of dispersion-managed soliton is in the order of fs, and the pulse width oscillates periodically. It is attributed to the imbalance of nonlinearity and dispersion in the net positive dispersion region, which also causes the periodic modulation of the self-imaging beat length $L_p$ in GIMF, and the periodic change of beat length leads to the fluctuation of coupling efficiency from GIMF to SMF. It indicates that the reverse saturable absorption of CA-GIMFs can suppress the high peak power of the pulses.

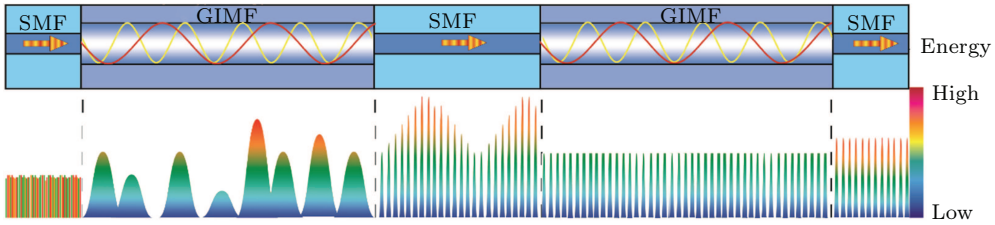



**Fig. 4.** The principle of dissipative soliton fiber laser based on CA-GIMFs ultrafast optical switch.

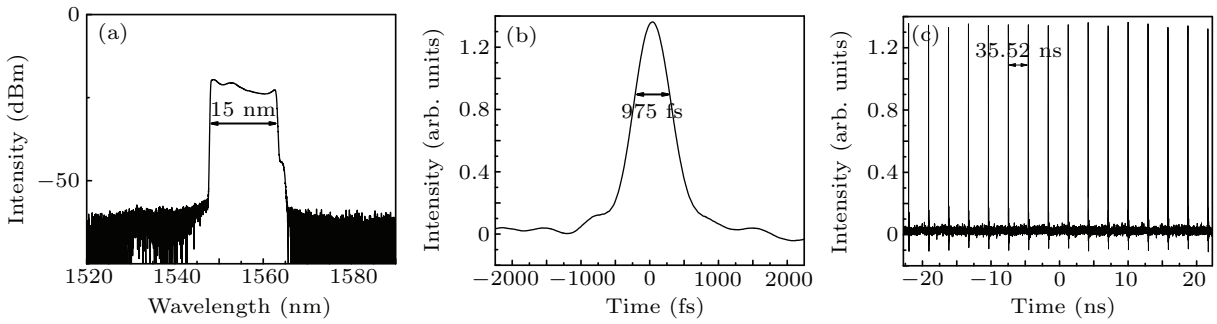



**Fig. 5.** Characteristics of the mode-locking pulses based on CA-GIMFs. (a) The optical spectrum, (b) autocorrelation trace of pulses, (c) the pulse train.

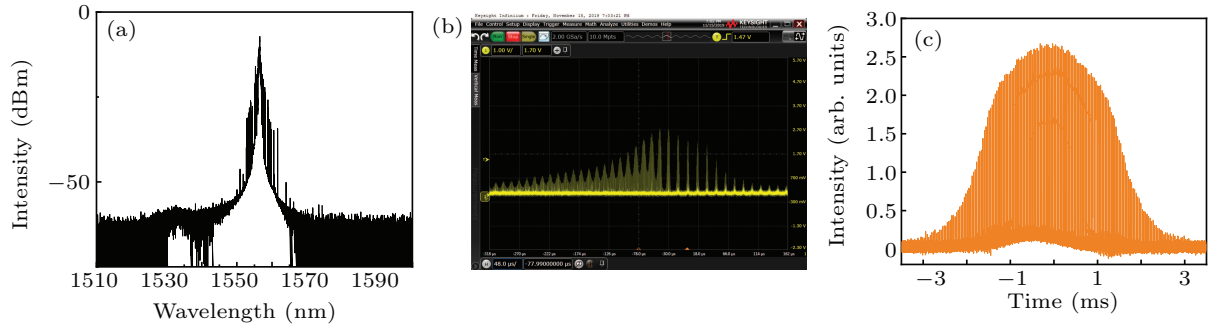



**Fig. 6.** Characteristics of the mode-locking pulses based on single GIMF: (a) optical spectrum, (b) the pulse train, (c) the envelop of mode-locking.

## 5. Conclusion

In this paper, the all-fiber dissipative soliton laser at 1.55 μm is realized based on the combination of saturable and reverse saturable absorption. In the experiment, a CA-GIMFs is employed to serve as an ultrafast optical switch. By fine tuning the PCs, the coupling efficiency between GIMF and SMF in CA-GIMFs is controlled, makes the CA-GIMFs have both saturable and reverse saturable absorption characteristics, and the modulation depths of saturable and reserve saturable absorption can reach 8.55% and −7.8%, respectively. The energy of the dissipative solitons is up to 0.41 nJ with the width of 975 fs, and the maximum average power is 11.48 mW. This method based on the combination of saturable and reserve saturable absorption nonlinear optical modulation properties provides a new idea for realizing soliton dissipation and increasing single pulse energy.

## References

[1] Cabasse A, Martel G and Oudar J L 2009 *Opt. Express* **17** 9537
[2] Lefranois S, Liu C H, Sosnowski T S, Galvanauskas A and Wise F W 2011 *Proceedings of SPIE - the International Society for Optical Engineering* **7914** 79141
[3] Li M, Zou X, Wu J, Shi J D, Qiu J F and Hong X B 2015 *Appl. Opt.* **54** 8800
[4] Liu X 2014 *General Assembly & Scientific Symposium IEEE*
[5] Yan D, Li X L, Zhang S M, Han M M, Han H Y and Yang Z J 2016 *Opt. Express* **24** 739
[6] Wang N, Cai J H, Qi X, Chen S P, Yang L J and Hou J 2018 *Opt. Express* **26** 1689
[7] Zhang H, Tang D Y, Wu X and Zhao L M 2009 *Opt. Express* **17** 12692
[8] Lee D, Park K, Debnath P C, Kim I and Song Y W 2016 *Nanotechnology* **27** 365203
[9] Zhao C J, Huang B, Liu J, Tang P H and Wen S C 2016 *Progress in Electromagnetic Research Symposium (PIERS) IEEE*

[10] Wang M, Zhu J, Zi Y, Wu Z G, Hu H, Xie Z, Zhang Y, Hu L and Huang W 2021 *J. Mater. Chem. A* **9** 12433
[11] Huang W, Zhu J, Wang M, Hu L, Tang Y, Shu Y, Xie Z and Zhang H 2020 *Adv. Funct. Mater.* **31** 2007584
[12] Huang W, Ma C, Li C, Zhang Y and Zhang H 2021 *Nanophotonics* **9** 8
[13] Huang W, Zhang Y, You Q, Hang P, Wang Y, Huang Z N, Ge Y, Wu L, Dong Z, Dai X, Xiang Y, Li J, Zhang X and Zhang H 2019 *Small* **15** 1900902
[14] Zhang J, Jiang T and Zhou T 2018 *Photon. Res.* **6** C8
[15] Nazemosadat E and Mafi A 2013 *J. Opt. Soc. Am. B* **30** 1357
[16] Fu S J, Sheng Q, Zhu X S, Shi W, Yao J Q, Shi G N, Norwood R A and Peyghambarian N 2015 *Opt. Express* **23** 17255
[17] Wang Z K, Wang D N, Fan Y, Li L J, Zhao C L, Xu B, Jin S Z, Cao S Y and Fang Z J 2018 *Opt. Lett.* **43** 2078
[18] Li H H, Wang Z K, Li C, Zhang J J and Xu S Q 2017 *Opt. Express* **25** 26546
[19] Yang F, Wang D N, Wang Z K, Li L J, Zhao C L, Xu B, Jin S Z, Cao S Y and Fang Z J 2018 *Opt. Express* **26** 927
[20] Chen H J, Liu M, Yao J, Hu S, He J B, Luo A P, Xu W C and Luo Z C 2018 *Opt. Express* **26** 2972
[21] Khattak A, Tatel G and Li W 2018 *Appl. Sci.* **8** 1135
[22] Zhan H W, Jin L, Zhang H, Xu Y T, Shi L L, Wang T B, Chen H C, Wang D T and Ma X H 2019 *Opt. Commun.* **452** 7
[23] Zhan H W, Jin L, Xu Y T, Zhang H, Shi L L, Wang T B, Pan W and Ma X H 2019 *Appl. Opt.* **58** 5788
[24] Wang T B, Jin L, Zhang H W, Pan W, Zhang H, Xu Y T, Shi L L, Li Y, Zou Y G and Ma X H 2020 *Ann. Phys.-Berlin* **532** 2000018
[25] Zhao Y, Jin Y and Liang H 2011 *Photonics & Optoelectronics IEEE*
[26] Hatta A M, Semenova Y, Rajan G and Farrell G 2012 *Opt. Laser Techn.* **42** 1044